

Nucleon form factors from basis light front quantization

Chandan Mondal^a, Siqi Xu^a, Jiangshan Lan^{a,b}, Xingbo Zhao^{a,b}, Yang Li^c,
Henry Lamm^d and James P. Vary^c

^a*Institute of Modern Physics, Chinese Academy of Sciences, Lanzhou 730000, China*

^b*University of Chinese Academy of Sciences, Beijing 100049, China*

^c*Department of Physics and Astronomy, Iowa State University, Ames, IA 50011, USA*

^d*Department of Physics, University of Maryland, College Park, Maryland 20742, USA*

Abstract

We investigate the electromagnetic form factors of the nucleon in the framework of basis light front quantization. We compute the form factors using the light front wavefunctions obtained by diagonalizing the effective Hamiltonian consisting of the holographic QCD confinement potential, the longitudinal confinement, and a one-gluon exchange interaction with fixed coupling. The electromagnetic radii of the nucleon are also computed.

Keywords: *Form factors; Light front quantization; Nucleon.*

1 Introduction

Electromagnetic form factors are critical to understanding nucleon structure. There are many experiments and theoretical studies on these form factors and they remain a very active field of research. We refer to the articles [1–5] for detailed reviews. It is well known that the matrix element of electromagnetic current for the nucleon requires two form factors namely Dirac and Pauli form factors,

$$J_{had}^\mu(q^2) = \bar{u}(p') \left(\gamma^\mu F_1(q^2) + \frac{i\sigma^{\mu\nu} q_\nu}{2M} F_2(q^2) \right) u(p), \quad (1)$$

where $q^2 = (p' - p)^2 = -2p' \cdot p + 2M^2 = -Q^2$ is the square of the momentum transferred to the nucleon and M is the nucleon mass. The normalizations of the form factors are given by $F_1^p(0) = 1$, $F_2^p(0) = \kappa_p = 1.793$ for the proton and $F_1^n(0) = 0$, $F_2^n(0) = \kappa_n = -1.913$ for the neutron. Cates et al. [6] first decomposed the nucleon form factors into their flavor components. Writing the hadronic current as the sum of quark currents one can decompose the nucleon electromagnetic form factors into flavor dependent form factors. Neglecting the strange quark contribution, the hadronic matrix element for electromagnetic current can be expressed as

$$J_{had}^\mu(q^2) = \langle N(p') | (e_u \bar{u} \gamma^\mu u + e_d \bar{d} \gamma^\mu d) | N(p) \rangle, \quad (2)$$

Proceedings of the International Conference ‘Nuclear Theory in the Supercomputing Era — 2018’ (NTSE-2018), Daejeon, South Korea, October 29 – November 2, 2018, eds. A. M. Shirokov and A. I. Mazur. Pacific National University, Khabarovsk, Russia, 2019, p. 1.

<http://www.ntse.khb.ru/2018/Proc/Mondal.pdf>.

where e_u and e_d are the charges of u and d quarks in units of positron charge(e). Under the charge and isospin symmetry $\langle p | \bar{u}\gamma^\mu u | p \rangle = \langle n | \bar{d}\gamma^\mu d | n \rangle$, it is straightforward to write down the flavor form factors in term of the nucleon form factors as

$$\begin{aligned} F_i^u(Q^2) &= 2F_i^p(Q^2) + F_i^n(Q^2), \\ F_i^d(Q^2) &= F_i^p(Q^2) + 2F_i^n(Q^2), \quad (i = 1, 2), \end{aligned} \quad (3)$$

with the normalizations $F_1^u(0) = 2$, $F_2^u(0) = \kappa_u$ and $F_1^d(0) = 1$, $F_2^d(0) = \kappa_d$ where the anomalous magnetic moments for the up and the down quarks are $\kappa_u = 2\kappa_p + \kappa_n = 1.673$ and $\kappa_d = \kappa_p + 2\kappa_n = -2.033$. It was shown in [6] that though the ratio of Pauli and Dirac form factors for the proton $F_2^p/F_1^p \propto 1/Q^2$, the Q^2 dependence is almost constant for the ratio of the quark form factors F_2/F_1 for both u and d . The Sachs form factors for the nucleon are written in terms of Dirac and Pauli form factors as

$$G_E^N(Q^2) = F_1^N(Q^2) - \frac{Q^2}{4M^2} F_2^N(Q^2), \quad (4)$$

$$G_M^N(Q^2) = F_1^N(Q^2) + F_2^N(Q^2), \quad (5)$$

and the electromagnetic radii are defined by

$$\langle r_E^2 \rangle^N = -6 \frac{dG_E^N(Q^2)}{dQ^2} \Big|_{Q^2=0}, \quad (6)$$

$$\langle r_M^2 \rangle^N = -\frac{6}{G_M^N(0)} \frac{dG_M^N(Q^2)}{dQ^2} \Big|_{Q^2=0}. \quad (7)$$

The basis light front quantization (BLFQ) approach has been developed for solving many-body bound state problems in quantum field theories [7, 8, 10, 13]. It is a Hamiltonian formalism incorporating the advantages of the light front dynamics [11, 12]. This formalism has been successfully applied to quantum electrodynamics (QED) systems including the electron anomalous magnetic moment [10] and the strong coupling bound-state positronium problem [8]. It has also been applied to heavy quarkonia [13–15] and B_c mesons [16] as QCD bound states. Recently, the BLFQ approach using a Hamiltonian that includes the color singlet Nambu-Jona-Lasinio interaction to account for the chiral dynamics has been applied to the light mesons [17–19]. In this work, we study the electromagnetic form factors of the nucleon using the light front wavefunctions (LFWFs) obtained by diagonalizing the effective light front Hamiltonian in the constituent valence quark representation with the potential including the light front holographic QCD in the transverse direction [20], longitudinal confinement [13], and one-gluon exchange interaction with a fixed coupling in the framework of BLFQ.

2 Effective light front Hamiltonian

The structures of the bound states are encoded in the LFWFs which are obtained as the eigenfunctions of the light front Schrödinger equation

$$H_{\text{eff}}|\Psi\rangle = M^2|\Psi\rangle, \quad (8)$$

where H_{eff} is the effective Hamiltonian of the system with the mass squared M^2 eigenvalue. In general, $|\Psi\rangle$ is the eigenvector in the Hilbert space spanned by all

Fock sectors. In the valence Fock sector, the effective Hamiltonian for the nucleon wavefunctions that we adopt is given by [21–23]

$$H_{\text{eff}} = \sum_a \frac{\vec{k}_{a\perp}^2 + m_a^2}{x_a} + \frac{1}{2} \sum_{a,b} \left[\kappa_T^4 x_a x_b (\vec{r}_{a\perp} - \vec{r}_{b\perp})^2 - \frac{\kappa_L^4}{(m_a + m_b)^2} \partial_{x_a} (x_a x_b \partial_{x_b}) \right] \\ + \frac{1}{2} \sum_{a,b} \frac{C_F 4\pi\alpha_s(Q_{ab}^2)}{Q_{ab}^2} \bar{u}_{s'_a}(k'_a) \gamma^\mu u_{s_a}(k_a) \bar{u}_{s'_b}(k'_b) \gamma^\nu u_{s_b}(k_b) d_{\mu\nu}, \quad (9)$$

where $\sum_a x_a = 1$, and $\sum_a \mathbf{k}_{a\perp} = 0$. $m_{a/b}$ is the mass of the quark, and κ_L (κ_T) is the strength of the longitudinal (transverse) confinement. $\vec{\zeta}_\perp \equiv \sqrt{x_a x_b} \vec{r}_\perp$ is the holographic variable [20], where $\vec{r}_\perp = \vec{r}_{a\perp} - \vec{r}_{b\perp}$ is the transverse separation between two quarks, $\partial_x f(x, \vec{\zeta}_\perp) = \partial f(x, \vec{\zeta}_\perp) / \partial x|_{\vec{\zeta}_\perp}$. $Q_{ab}^2 = -q^2 = -(1/2)(k'_a - k_a)^2 - (1/2)(k'_b - k_b)^2$ is the average momentum transfer squared, $C_F = -2/3$ is the color factor. $d_{\mu\nu}$ is the gluon polarization tensor which reduces to the metric tensor $g_{\mu\nu}$ by summing over the dynamical one-gluon exchange and the instantaneous gluon exchange and α_s is the running coupling which can be replaced by a constant for simplicity. Note that we use different quark masses in the kinetic energy term and in the one gluon exchange interaction of the effective light front Hamiltonian to simulate the effects of higher Fock components and the other QCD interactions. Upon diagonalization of the resulting sparse effective Hamiltonian matrix in a chosen basis representation, one obtains the mass spectrum and corresponding wavefunctions of the system.

In BLFQ, Eq. (8) is expressed in a truncated basis representation of the valence Fock space, and the resulting finite-dimensional matrix is diagonalized numerically. The choice of basis is arbitrary as long as it is orthogonal and normalized. We choose the two dimensional harmonic oscillator (‘2D-HO’) basis in the transverse direction and the discretized plane-wave basis in the longitudinal direction [7,8,10,13]. Each single-particle basis state can be identified using four quantum numbers, $\bar{\alpha} = \{k, n, m, \lambda\}$. The longitudinal momentum of the particle is characterized by the first quantum number k . In the longitudinal direction x^- , we constrain the system to a box of length $2L$, and impose (anti-) periodic boundary conditions on (fermions) bosons. As a result, the longitudinal momentum $p^+ = 2\pi k/L$ is discretized, where the dimensionless quantity $k = 1, 2, 3, \dots$ for bosons and $k = \frac{1}{2}, \frac{3}{2}, \frac{5}{2}, \dots$ for fermions. The zero mode for bosons is neglected. In the many-body basis, all basis states are selected to have the same total longitudinal momentum $P^+ = \sum_i p_i^+$, where the sum is over the particles in a particular basis state. One then parameterizes P^+ using a dimensionless variable $K = \sum_i k_i$ such that $P^+ = \frac{2\pi}{L} K$. For a given particle i , the longitudinal momentum fraction x is defined as

$$x_i = \frac{p_i^+}{P^+} = \frac{k_i}{K}. \quad (10)$$

K determines the “resolution” in the longitudinal direction, and thus the resolution on parton distribution functions. The longitudinal continuum limit corresponds to the limit $L, K \rightarrow \infty$. The next two quantum numbers, n and m , denote radial excitation and angular momentum projection, respectively, of the particle within the 2D-HO basis in the transverse direction. The choice of the 2D HO basis for BLFQ is made because the HO potential is a confining potential, and therefore its wavefunctions should form an ideal basis for systems subject to QCD confinement. Since we assume

harmonic confinement in the transverse direction, these transverse basis states are also computationally convenient.

In order to numerically diagonalize H_{eff} , the infinite dimensional basis must be truncated down to a finite dimension. In BLFQ, two levels of truncation scheme are implemented. First, the number of Fock sectors in the basis is restricted. This truncation will be based on physical as well as practical considerations. For instance, the nucleon is expected to be fairly well described by the lowest few sectors. For example, the nucleon state can be expressed schematically as

$$|N\rangle_{\text{phys}} = a|qqq\rangle + b|qqqq\rangle + c|qqqq\bar{q}\rangle + \dots \quad (11)$$

In this work, we limit ourselves to only the leading Fock sector $|qqq\rangle$.

Second, within each Fock-sector, further truncation is still needed to reduce the basis to a finite dimension. We introduce a truncation parameter K_{max} on the longitudinal direction such that, $\sum_l k_l \leq K_{\text{max}}$, where k_l is the longitudinal momentum quantum number of l -th particle in the basis state. Note that systems with larger K_{max} have simultaneously higher ultra-violet (UV) and lower infra-red (IR) cutoffs in the longitudinal direction. In the transverse direction, we require the total transverse quantum number $N_\alpha = \sum_l (2n_l + |m_l| + 1)$ for multi-particle basis state $|\alpha\rangle$ satisfies $N_\alpha \leq N_{\text{max}}$, where N_{max} is a chosen truncation parameter. The transverse continuum limit corresponds to $N_{\text{max}} \rightarrow \infty$. The 2D-HO basis may be defined by two parameters, mass M and frequency Ω . We adopt a single HO parameter $b = \sqrt{M\Omega}$, since our transverse modes depend only on b rather than on M and Ω individually. Here, we choose the value of $b = 0.45$ GeV, the same as the confining strength $\kappa_L(\kappa_T)$. N_{max} and b define both the transverse IR and UV regulator in BLFQ. In addition, our many body states have well defined values of the total angular momentum projection $M_J = \sum_i (m_i + \lambda_i)$, where λ is the fourth quantum number which corresponds the helicity of the particle.

3 Electromagnetic form factors in BLFQ

In the light front formalism for a spin $\frac{1}{2}$ composite system the Dirac and Pauli form factors $F_1(q^2)$ and $F_2(q^2)$ are identified with the helicity-conserving and helicity-flip matrix elements of the J^+ current [25]

$$\langle P+q, \uparrow | \frac{J^+(0)}{2P^+} | P, \uparrow \rangle = F_1(q^2), \quad (12)$$

$$\langle P+q, \uparrow | \frac{J^+(0)}{2P^+} | P, \downarrow \rangle = -(q^1 - iq^2) \frac{F_2(q^2)}{2M}, \quad (13)$$

where M is the nucleon mass and the arrow indicates the helicity of the nucleon. The physical nucleon state with momentum P can be expanded in terms of multi-particle light front wavefunctions [26]:

$$\begin{aligned} |P, S_z\rangle = & \sum_n \int \prod_{i=1}^n \frac{dx_i d^2k_{\perp i}}{\sqrt{x_i} 16\pi^3} 16\pi^3 \delta\left(1 - \sum_{i=1}^n x_i\right) \delta^2\left(\sum_{i=1}^n k_{\perp i}\right) \\ & \times \psi_n^{S_z}(x_i, k_{\perp i}, \lambda_i) |n, x_i P^+, x_i P_\perp + k_{\perp i}, \lambda_i\rangle; \end{aligned} \quad (14)$$

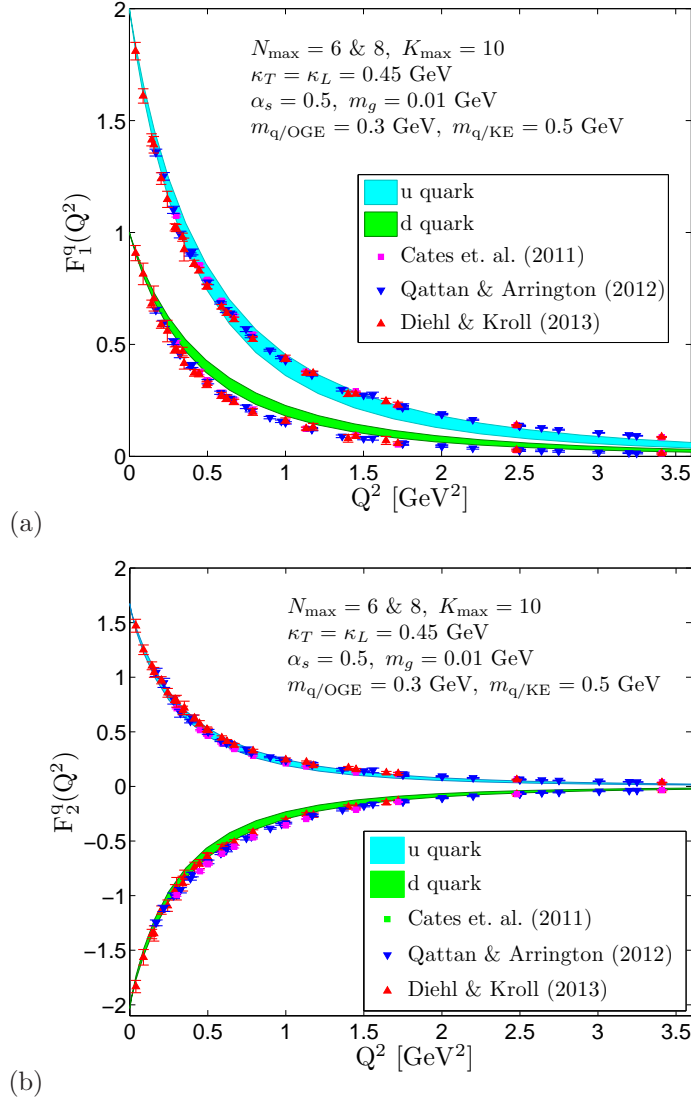


Figure 1: (Color online) BLFQ results for (a) the Dirac and, (b) the Pauli form factors of u and d quarks with confining strength, $\kappa_L = \kappa_T = 0.45$ GeV and fixed coupling $\alpha_s = 0.5$. The quark mass in the kinetic energy term is $m_{q/\text{KE}} = 0.5$ GeV, whereas the quark mass in one gluon exchange interaction is $m_{q/\text{OGE}} = 0.3$ GeV. The bands correspond the range for $N_{\text{max}} = 6 - 8$ with $K_{\text{max}} = 10$. We choose the value of HO parameter b same as $\kappa_L(\kappa_T)$ i.e. $b = 0.45$ GeV. $m_g (= 0.01$ GeV) is a small gluon mass regulator used for numerical convenience. The experimental data are taken from [6, 27, 28].

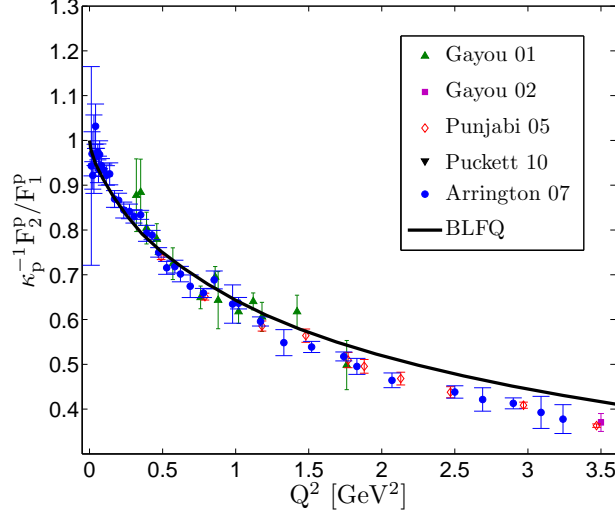


Figure 2: (Color online) The ratio of Pauli and Dirac form factors of the proton with the same parameters as mentioned in Fig. 1 and with basis truncation $N_{\text{max}} = 8$ and $K_{\text{max}} = 10$. The ratio is divided by κ_p . The experimental data are taken from Refs. [29–33].

here $x_i = k_i^+ / P^+$ and $k_{\perp i}$ represent the relative transverse momentum of the i -th constituent and n is the number of particles in a Fock state. The physical transverse momenta are $p_{\perp i} = x_i P_{\perp} + k_{\perp i}$. λ_i and S_z are the light-cone helicities of the quark and nucleon, respectively. The boost invariant light-front wave functions ψ_n depend only on x_i and $k_{\perp i}$ and are independent of the total momentum of the state P^+ and P_{\perp} . In the overlap representation, the electromagnetic form factors are then expressed as

$$F_1^q(q^2) = \sum_{n, \lambda_i} \int \prod_{i=1}^n \frac{dx_i d^2 k_{\perp i}}{16\pi^3} 16\pi^3 \delta \left(1 - \sum_j x_j \right) \delta^2 \left(\sum_{j=1}^n k_{\perp j} \right) \times \psi_n^{\uparrow*}(x'_i, k'_{\perp i}, \lambda_i) \psi_n^{\uparrow}(x_i, k_{\perp i}, \lambda_i); \quad (15)$$

$$\frac{-(q^1 - iq^2)}{2M} F_2^q(q^2) = \sum_{n, \lambda_i} \int \prod_{i=1}^n \frac{dx_i d^2 k_{\perp i}}{16\pi^3} 16\pi^3 \delta \left(1 - \sum_j x_j \right) \delta^2 \left(\sum_{j=1}^n k_{\perp j} \right) \times \psi_n^{\uparrow*}(x'_i, k'_{\perp i}, \lambda_i) \psi_n^{\downarrow}(x_i, k_{\perp i}, \lambda_i); \quad (16)$$

where for the struck parton $x'_1 = x_1$; $k'_{\perp 1} = k_{\perp 1} + (1 - x_1)q_{\perp}$ and $x'_i = x_i$; $k'_{\perp i} = k_{\perp i} - x_i q_{\perp}$ for the spectators ($i = 2, \dots, n$). We consider the frame where $q = (0, 0, \mathbf{q}_{\perp})$, thus $Q^2 = -q^2 = \mathbf{q}_{\perp}^2$. Since we restrict ourselves to the leading Fock sector, the nucleon basis state can be written as

$$|N_{\text{phys}}^{S_z}\rangle = |k_{q_1}, n_{q_1}, m_{q_1}, \lambda_{q_1}\rangle \otimes |k_{q_2}, n_{q_2}, m_{q_2}, \lambda_{q_2}\rangle \otimes |k_{q_3}, n_{q_3}, m_{q_3}, \lambda_{q_3}\rangle. \quad (17)$$

We obtain the light front wavefunctions numerically by diagonalizing the effective Hamiltonian given in Eq.(9) with the basis representation given by Eq. (17). Using the

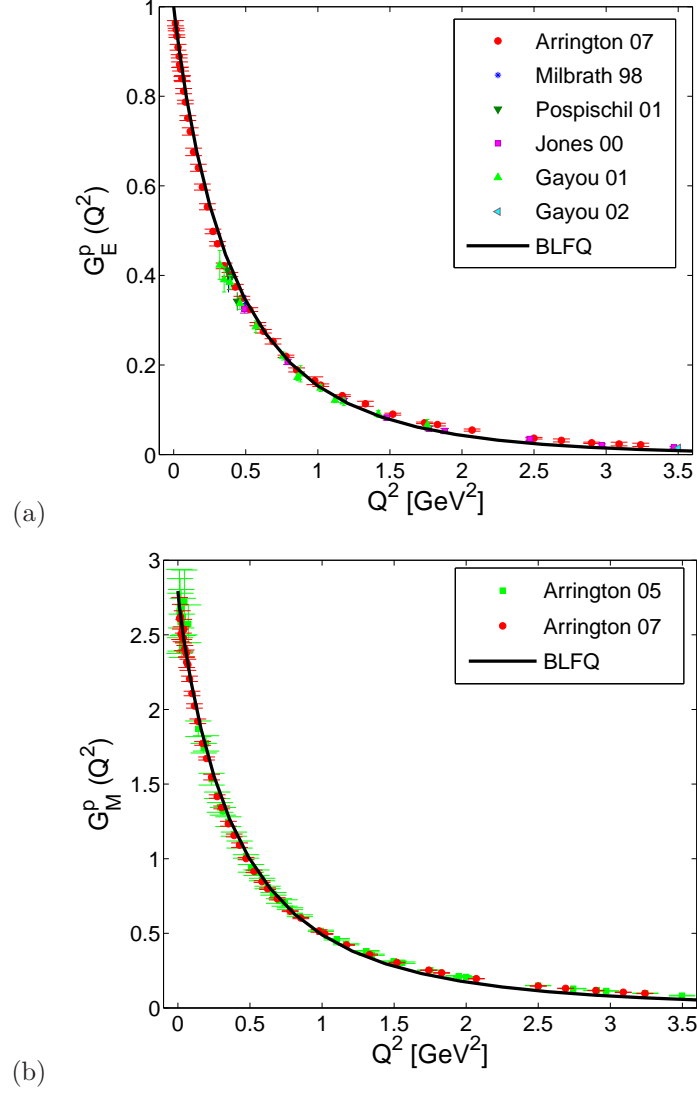


Figure 3: (Color online) (a) BLFQ results for the Sachs form factors (a) $G_E(Q^2)$, and (b) $G_M(Q^2)$ of the proton with the same parameters as mentioned in Fig. 1 and with basis truncation $N_{\text{max}} = 8$ and $K_{\text{max}} = 10$. The experimental data are taken from Refs. [29–31, 34–36] and [31, 37].

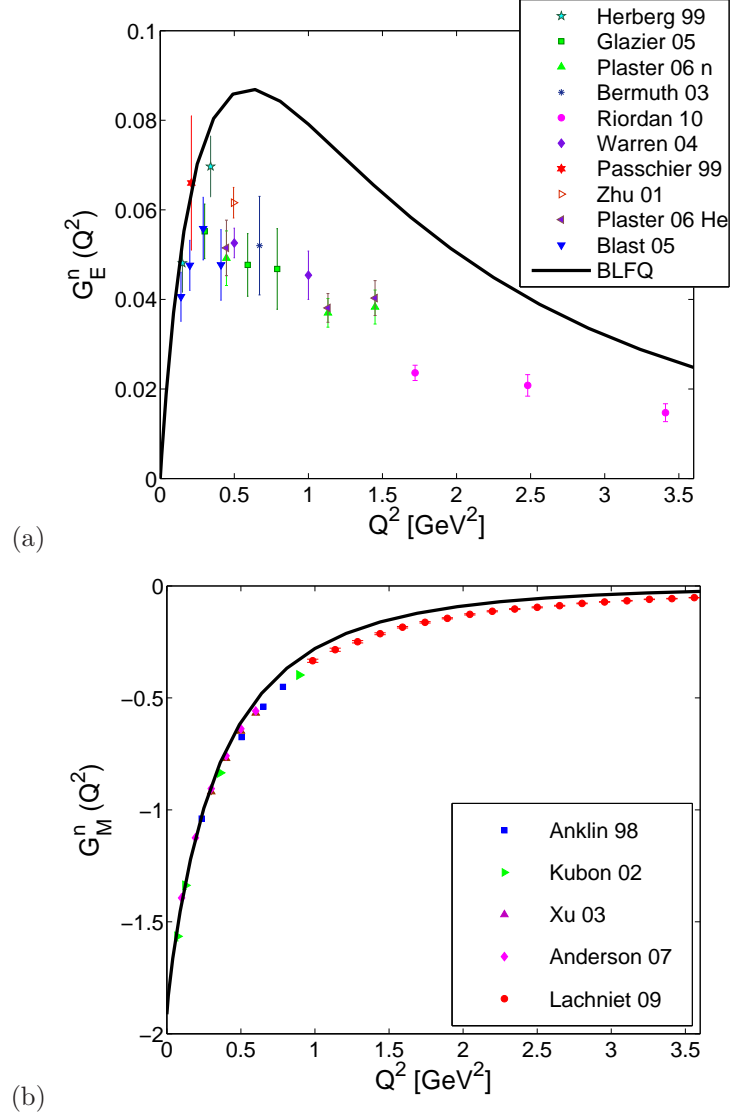


Figure 4: (Color online) (a)BLFQ results for the Sachs form factors (a) $G_E(Q^2)$, and (b) $G_M(Q^2)$ of the neutron with the same parameters as mentioned in Fig. 1 and with basis truncation $N_{\text{max}} = 8$ and $K_{\text{max}} = 10$. The experimental data are taken from Refs. [29–31, 34–36] and [39–43].

resulting light front wavefunctions ψ_n , we evaluate the electromagnetic form factors of the nucleon. The parameters are tuned to fit the electromagnetic properties of the nucleons. Following the convention of [24], we fix the normalizations of the Dirac and the Pauli form factors as

$$F_1^q(Q^2) = n_q \frac{F_1^{(\text{BLFQ})q}(Q^2)}{F_1^{(\text{BLFQ})q}(0)}, \quad F_2^q(Q^2) = \kappa_q \frac{F_2^{(\text{BLFQ})q}(Q^2)}{F_2^{(\text{BLFQ})q}(0)}, \quad (18)$$

so that $F_1^q(0) = n_q$ and $F_2^q(0) = \kappa_q$ where $n_u = 2$, $n_d = 1$ and the anomalous magnetic moments for the u and d quarks are $\kappa_u = 1.673$ and $\kappa_d = -2.033$. The advantage of the modified formulae in Eq.(18) is that, irrespective of the values of the parameters, the normalization conditions for the form factors are automatically satisfied.

In Fig. 1, we show the Q^2 dependence of the Dirac and the Pauli form factors of u and d quark. We set the confining strength, $\kappa_L = \kappa_T = 0.45$ GeV in both the longitudinal and transverse confinements and the coupling constant $\alpha_s = 0.5$. The bands represent the range of our results due to increasing the basis from $N_{\text{max}} = 6$ to $N_{\text{max}} = 8$ with $K_{\text{max}} = 10$. We use different quark masses i.e. in the kinetic energy term, $m_{q/\text{KE}} = 0.5$ GeV and in the one gluon exchange interaction, $m_{q/\text{OGE}} = 0.3$ GeV in order to minimize the effect of higher Fock component and the other QCD interactions. Fig. 1 shows that the BLFQ results for the flavor Pauli form factors are in reasonable agreement with the experimental data. The Dirac form factor for the u quark is also in reasonable agreement with the data. However, the theoretical d quark form factor is somewhat over estimated compared to the data.

The nucleon form factors can be obtained from the flavor dependent form factors. The ratio of Pauli and Dirac form factors of the proton for $N_{\text{max}} = 8$ and $K_{\text{max}} = 10$ is shown in Fig. 2. We find that at low Q^2 our result agrees well with the experimental data. The Sachs form factors for the proton are presented in Fig. 3 where we find a good agreement between theory and experiment. In Fig. 4, we show the Sachs form factors for the neutron. Our results for the neutron magnetic form factor is in reasonable agreement with experimental data, however, for the charge form factor is over estimated compared to the data. The deviations of the neutron charge form factor from the experimental data can be attributed to the fact that the d quark form factor F_1^d does not have the correct behavior in this model. From the Sachs form factors we also compute the electromagnetic radii of the nucleons. We quote the radii in Table 1, the experimental values are taken from the Ref. [38]. Here again, we find reasonable agreement with experiment.

Quantity	BLFQ	Measured data [38]
r_E^p	0.804 fm	0.877 ± 0.005 fm
r_M^p	0.917 fm	0.777 ± 0.016 fm
$\langle r_E^2 \rangle^n$	-0.1214 fm^2	$-0.1161 \pm 0.0022 \text{ fm}^2$
r_M^n	1.007 fm	$0.862^{+0.009}_{-0.008}$ fm

Table 1: Electromagnetic radii of the nucleons.

4 Conclusions

The electromagnetic form factors for the nucleon and their flavor decomposition have been presented using the BLFQ approach. The form factors have been evaluated from the overlaps of the light front wavefunctions which were obtained by diagonalizing the effective Hamiltonian. In our model, we consider the holographic QCD confinement potential, longitudinal confinement, and a one-gluon exchange interaction with fixed coupling in the effective light front Hamiltonian. We observed a reasonable agreement of our results for the proton and u quark form factors with the experimental data, however, for the Dirac form factor of d quark and the neutron charge form factors deviate from the data for the basis truncation $N_{\text{max}} = 8$ and $K_{\text{max}} = 10$. We also presented the electromagnetic radii for the nucleon.

Acknowledgments: CM is supported by the China Postdoctoral Science Foundation (CPSF) under the Grant No. 2017M623279 and the National Natural Science Foundation of China (NSFC) under the Grant No. 11850410436. This work of XZ is supported by new faculty startup funding by the Institute of Modern Physics, Chinese Academy of Sciences under the Grant No. Y632030YRC. HL is supported by the U.S. Department of Energy under Award No. DE-FG02-93ER-40762. This work of JPV is supported by the Department of Energy under Grants Nos. DE-FG02-87ER40371, DE-SC0018223 (SciDAC4/NUCLEI), and DE-SC0015376 (DOE Topical Collaboration in Nuclear Theory for Double-Beta Decay and Fundamental Symmetries).

References

- [1] H. Y. Gao, Int. J. Mod. Phys. E **12**, 1 (2003).
- [2] C. E. Hyde-Wright and K. de Jager, Ann. Rev. Nucl. Part. Sci. **54**, 217 (2004).
- [3] C. F. Perdrisat, V. Punjabi and M. Vanderhaeghen, Prog. Part. Nucl. Phys. **59**, 694 (2007).
- [4] D. Chakrabarti and C. Mondal, Eur. Phys. J. C **73**, 2671 (2013).
- [5] C. Mondal, Phys. Rev. D **94**, no. 7, 073001 (2016).
- [6] G. D. Cates, C. W. de Jager, S. Riodian and B. Wojtsekhowski, Phys. Rev. Lett. **106**, 252003 (2011).
- [7] J. P. Vary *et al.*, Phys. Rev. C **81**, 035205 (2010).
- [8] P. Wiecki, Y. Li, X. Zhao, P. Maris and J. P. Vary, Phys. Rev. D **91**, no. 10, 105009 (2015).
- [9] Y. Li, P. Maris, X. Zhao and J. P. Vary, Phys. Lett. B (2016).
- [10] X. Zhao, H. Honkanen, P. Maris, J. P. Vary and S. J. Brodsky, Phys. Lett. B **737**, 65 (2014).
- [11] S. J. Brodsky, H. C. Pauli and S. S. Pinsky, Phys. Rept. **301**, 299 (1998).

- [12] J. R. Hiller, Prog. Part. Nucl. Phys. **90**, 75 (2016).
- [13] Y. Li, P. Maris, X. Zhao and J. P. Vary, Phys. Lett. B (2016).
- [14] Y. Li, P. Maris and J. P. Vary, Phys. Rev. D **96**, no. 1, 016022 (2017).
- [15] J. Lan, C. Mondal, M. Li, Y. Li, S. Tang, X. Zhao and J. P. Vary, arXiv:1911.11676 [nucl-th].
- [16] S. Tang, Y. Li, P. Maris and J. P. Vary, arXiv:1810.05971 [nucl-th].
- [17] S. Jia and J. P. Vary, Phys. Rev. C **99**, no. 3, 035206 (2019).
- [18] J. Lan, C. Mondal, S. Jia, X. Zhao and J. P. Vary, Phys. Rev. Lett. **122**, no. 17, 172001 (2019).
- [19] J. Lan, C. Mondal, S. Jia, X. Zhao and J. P. Vary, arXiv:1907.01509 [nucl-th].
- [20] S. J. Brodsky, G. F. de Teramond, H. G. Dosch and J. Erlich, Phys. Rept. **584**, 1 (2015).
- [21] C. Mondal, S. Xu, J. Lan, X. Zhao, Y. Li, D. Chakrabarti and J. P. Vary, arXiv:1911.10913 [hep-ph].
- [22] C. Mondal, S. Xu, J. Lan, X. Zhao, Y. Li, H. Lamm and J. P. Vary, PoS DIS **2019**, 190 (2019).
- [23] C. Mondal, S. Xu, J. Lan, X. Zhao, Y. Li, D. Chakrabarti and J. P. Vary, arXiv:2001.04414 [hep-ph].
- [24] C. Mondal and D. Chakrabarti, Eur. Phys. J. C **75**, no. 6, 261 (2015).
- [25] S. J. Brodsky and S. D. Drell, Phys. Rev. D **22**, 2236 (1980).
- [26] S. J. Brodsky, M. Diehl, D. S. Hwang, Nucl. Phys. B **596**, 99 (2001).
- [27] I. A. Qattan and J. Arrington, Phys. Rev. C **86**, 065210 (2012).
- [28] M. Diehl and P. Kroll, Eur. Phys. J. C **73**, 2397 (2013).
- [29] O. Gayou *et. al.*, Phys. Rev. C **64**, 038202 (2001).
- [30] O. Gayou *et. al.*, Phys. Rev. Lett. **88**, 092301 (2002).
- [31] J. Arrington, W. Melnitchouk and J. A. Tjon, Phys. Rev. C **76**, 035205 (2007).
- [32] V. Punjabi *et. al.*, Phys. Rev. C **71**, 055202 (2005).
- [33] A. Puckett *et. al.*, Phys. Rev. Lett. **104**, 242301 (2010).
- [34] T. Pospischil *et. al.*, Eur. Phys. J. A **12**, 125 (2001).
- [35] B. D. Milbrath *et. al.*, Phys. Rev. Lett. **80**, 452 (1998).
- [36] M. K. Jones *et. al.*, Phys. Rev. Lett. **84**, 1398 (2000).
- [37] J. Arrington, Phys. Rev. C **71**, 015202 (2005).

- [38] J. Beringer et. al.(Particle data Group), Phys. Rev. D. **86**, 010001 (2012).
- [39] H. Anklin *et. al.*, Phys. Lett. B **428**, 248 (1998).
- [40] G. Kubon *et. al.*, Phys. Lett. B **524**, 26 (2002).
- [41] W. Xu *et. al.*, Phys. Rev. C **67**, 012201 (2003).
- [42] B. Anderson *et. al.*, Phys. Rev. C **75**, 034003 (2007).
- [43] J. Lachniet *et. al.*, Phys. Rev. Lett. **102**, 192001 (2009).